MCB
Journals.ASM.org

Loss of PTPN12 Stimulates Progression of ErbB2-Dependent Breast Cancer by Enhancing Cell Survival, Migration, and Epithelial-to-Mesenchymal Transition

Juan Li,[a] Dominique Davidson,[a] Cleiton Martins Souza,[a] Ming-Chao Zhong,[a] Ning Wu,[a] Morag Park,[b,c] William J. Muller,[b,c] André Veillette[a,d,e]

Laboratory of Molecular Oncology, Clinical Research Institute of Montréal, Montréal, Québec, Canada[a]; Goodman Cancer Centre, McGill University, Montréal, Québec, Canada[b]; Department of Biochemistry, McGill University, Montréal, Québec, Canada[c]; Department of Medicine, McGill University, Montréal, Québec, Canada[d]; Department of Medicine, University of Montréal, Montréal, Québec, Canada[e]

PTPN12 is a cytoplasmic protein tyrosine phosphatase (PTP) reported to be a tumor suppressor in breast cancer, through its capacity to dephosphorylate oncogenic receptor protein tyrosine kinases (PTKs), such as ErbB2. However, the precise molecular and cellular impact of PTPN12 deficiency in breast cancer progression remains to be fully clarified. Here, we addressed this issue by examining the effect of PTPN12 deficiency on breast cancer progression *in vivo*, in a mouse model of ErbB2-dependent breast cancer using a conditional PTPN12-deficient mouse. Our studies showed that lack of PTPN12 in breast epithelial cells accelerated breast cancer development and lung metastases *in vivo*. PTPN12-deficient breast cancer cells displayed enhanced tyrosine phosphorylation of the adaptor Cas, the adaptor paxillin, and the kinase Pyk2. They exhibited no detectable increase in ErbB2 tyrosine phosphorylation. PTPN12-deficient cells were more resistant to anoikis and had augmented migratory and invasive properties. Enhanced migration was corrected by inhibiting Pyk2. PTPN12-deficient breast cancer cells also acquired partial features of epithelial-to-mesenchymal transition (EMT), a feature of more aggressive forms of breast cancer. Hence, loss of PTPN12 promoted tumor progression in a mouse model of breast cancer, supporting the notion that PTPN12 is a tumor suppressor in human breast cancer. This function was related to the ability of PTPN12 to suppress cell survival, migration, invasiveness, and EMT and to inhibit tyrosine phosphorylation of Cas, Pyk2, and paxillin. These findings enhance our understanding of the role and mechanism of action of PTPN12 in the control of breast cancer progression.

Protein tyrosine phosphatases (PTPs) play a key role in normal cellular processes, such as proliferation, migration, adhesion, differentiation, and immune cell activation (1–3). Depending on the phosphatase and the cell type, they also have the ability either to suppress or to promote malignant transformation (3). PTPN12, also referred to as PTP-PEST (PTP—proline, glutamic acid, serine, and threonine rich), is a cytoplasmic PTP expressed in a wide spectrum of cell types (4). Studies of PTPN12-deficient mice showed that PTPN12 is a critical positive regulator of migration and adhesion in embryonic fibroblasts, endothelial cells, T cells, macrophages, and dendritic cells (5–11). This function relates to the capacity of PTPN12 to dephosphorylate cytoskeleton-associated substrates such as protein tyrosine kinases (PTKs) Pyk2 and FAK or the adaptors Cas, paxillin, and PSTPIP-1. These substrates are components of the cellular machinery controlling migration and adhesion. PTPN12 can also regulate other substrates, including receptor PTKs, such as ErbB2 and the adaptor Shc (12–14). Proteomic data suggested that the ability of PTPN12 to regulate Shc might be critical for conversion of Shc-dependent proliferative signals into migratory signals (15). Several PTPN12 substrates, and in particular, Cas, paxillin, and Shc, also directly associate with PTPN12.

Various studies have indicated that PTPN12 is a tumor suppressor. Sun et al. provided evidence that PTPN12 is a tumor suppressor for human breast cancer (14). In a small hairpin RNA (shRNA) screen targeting kinases and phosphatases in human mammary epithelial cells (HMECs), they observed that downregulation of PTPN12 expression triggered anchorage-independent growth and loss of acinar structure. These effects were accompanied by enhanced tyrosine phosphorylation of a variety of cellular proteins, including oncogenic receptor PTKs such as ErbB2, epidermal growth factor receptor (EGFR), and platelet-derived growth factor receptor (PDGFR), as well as the adaptor Cas. Those authors also observed that PTPN12-deficient human breast cancer cells grew more rapidly in transplanted xenogeneic mouse models. Lastly, they documented frequent loss of PTPN12 in human breast cancer cell lines and samples, as a result of point mutations, large deletions, altered microRNA expression, or reduced protein expression. These changes were more commonly seen in triple-negative breast cancer (TNBC), an aggressive subtype of breast cancer.

In support of the tumor suppressor role of PTPN12, at least two others groups also documented loss of PTPN12 protein in human breast cancer using immunohistochemistry or immunoblot analyses (16, 17). This alteration was more common in TNBC. Likewise, decreased expression of PTPN12 was reported in

Received 28 July 2015 **Returned for modification** 28 August 2015
Accepted 17 September 2015
Accepted manuscript posted online 21 September 2015
Citation Li J, Davidson D, Martins Souza C, Zhong M-C, Wu N, Park M, Muller WJ, Veillette A. 2015. Loss of PTPN12 stimulates progression of ErbB2-dependent breast cancer by enhancing cell survival, migration, and epithelial-to-mesenchymal transition. Mol Cell Biol 35:4069–4082. doi:10.1128/MCB.00741-15.
Address correspondence to André Veillette, andre.veillette@ircm.qc.ca.

other human malignancies, including non-small-cell lung carcinoma, esophageal squamous cell carcinoma, nasopharyngeal carcinoma, and hepatocellular carcinoma (18–21). In all cases, loss of PTPN12 correlated with aggressiveness and poor prognosis.

Despite the compelling evidence that PTPN12 acts as a tumor suppressor in human breast cancer, the precise molecular and cellular mechanisms of this activity remain to be fully understood. In particular, the demonstration that PTPN12 has a tumor suppressor function in a nonxenogeneic *in vivo* cancer model is important. Moreover, as PTPN12 is typically viewed as a regulator of cytoskeleton-associated substrates, rather than receptor PTKs, the nature of the targets on PTPN12 in an *in vivo* setting needs to be examined. Whether PTPN12 influences processes such as proliferation, cell survival, migration, and invasion should also be addressed. Finally, the basis for the more frequent association of loss of PTPN12 with aggressive tumor types should be clarified.

To understand these issues, the impact of PTPN12 deficiency was examined in a mouse model of ErbB2-driven breast cancer, a model of luminal-type breast cancer. This model was chosen because we wanted to test the possibility that loss of PTPN12 is involved in progression of breast cancer from less aggressive (such as luminal-type cancer) to more aggressive (such as TNBC) subtypes of breast cancer. This might explain why PTPN12 deficiency is more frequently seen in the more aggressive TNBC. By crossing this mouse with a breast epithelial cell-specific PTPN12-deficient mouse, we found that loss of PTPN12 enhanced breast cancer development and metastasis *in vivo*. These changes were associated with increased tyrosine phosphorylation of Cas, Pyk2, and paxillin but not ErbB2. PTPN12-deficient breast cancer cells had augmented migration and invasiveness and decreased susceptibility to anchorage-independent death (known as anoikis). Enhanced migration was corrected by inhibition of Pyk2. Compared to breast cancer cells from PTPN12-expressing mice, PTPN12-deficient breast cancer cells displayed more extensive features of epithelial-to-mesenchymal transition (EMT). These findings yield a better understanding of the mechanisms by which loss of PTPN12 accelerates breast cancer progression.

MATERIALS AND METHODS

Mice. The conditional allele of *Ptpn12* (*Ptpn12*$^{fl/fl}$) was previously described (7). MMTV-NIC (MMTV-*Neu*-IRES-*Cre*, where IRES is internal ribosome entry site) mice are described elsewhere (22).

Detection of breast tumors and metastases. Female mice were monitored for mammary tumor formation by weekly palpation. Mice were routinely sacrificed 5 weeks after tumors were initially discovered, at which time tumor volume, tumor weight, and extent of lung metastases were determined. Tumor volume and weight were measured as reported (23). For quantitation of lung metastases, lungs were fixed overnight at 4°C in 4% (vol/vol) paraformaldehyde (EMD Millipore, Etobicoke, Canada). Serial lung sections (100 μm per lung) were then obtained and analyzed by staining with hematoxylin and eosin (H&E). Metastases (defined as clusters of 10 cells or more) were detected by microscopy. Lesions present in multiple sections were counted only once.

Tumor-derived cell lines. Tumor-derived breast cancer cell lines were established from primary tumors by digesting tissues at 37°C for 2 to 4 h with dispase and collagenase D (2.5 mg/ml; Roche, Switzerland). After overnight culture in medium containing 10% fetal bovine serum, cells were maintained in serum-free Dulbecco modified Eagle medium supplemented with mammary epithelial cell growth supplement (MEGS; Wisent Bioproducts, St-Bruno, Canada) and insulin-transferrin-selenium (ITS; Gibco, NY). Medium was replaced every 2 days. To restore expression of PTPN12 in PTPN12-deficient cell lines, a mouse *Ptpn12* cDNA was inserted into the retroviral vector pMigR1, which also encodes green fluorescent protein (GFP). Production of retroviruses, retroviral infection, and selection of infected cells by sorting for GFP-positive cells were performed as detailed elsewhere (24).

Immunoprecipitations and immunoblots. To generate lysates from tumors, samples of similar volumes were ground in liquid nitrogen using a mortar and pestle. Tissues were then lysed with TNE buffer (50 mM Tris [pH 8.0], 150 mM NaCl, 1% NP-40, 2 mM EDTA [pH 8.0]) supplemented with phosphatase and protease inhibitors, as described previously (25). Tumor-derived cell lines were lysed by addition of lysis buffer directly to tissue culture dishes. Immunoprecipitation and immunoblotting were performed as reported elsewhere (25). Quantifications of protein bands in autoradiograms were analyzed using Gel-Pro Analyzer software (Media Cybernetics, Rockville, MD).

The following antibodies were used: anti-PTPN12 (generated in André Veillette's lab), anti-Fyn (generated in André Veillette's lab), anti-phospho-Cas (Tyr410; no. 4011; Cell Signaling), anti-Cas (no. sc-860; Santa Cruz), anti-phospho-Pyk2 (Tyr402; no. 3291; Cell Signaling), anti-Pyk2 (no. 3292, Cell Signaling), antipaxillin (no. 610052; BD Biosciences), anti-FAK (no. 610088; BD Biosciences), anti-phospho-FAK (Tyr397; no. 3283; Cell Signaling), anti-phospho-Neu (ErbB2) (Tyr1248; no. sc-12352-R; Santa Cruz), anti-Neu (ErbB2; no. sc-284; Santa Cruz), anti-Shc (generated in André Veillette's lab), antiphosphotyrosine (4G10; no. 05-321; Millipore), anti-phospho-Src (Tyr416; no. 2101; Cell Signaling), anti-Src MAb 327 (generated in André Veillette's lab), anti-phospho-Akt (Thr308; no. 9275; Cell Signaling), anti-Akt, 1:1,000 (no. 9272; Cell Signaling), anti-phospho-glycogen synthase kinase 3β (anti-phospho-GSK3β) (Ser9; no. 9322; Cell Signaling), anti-GSK3β (no. 9315; Cell Signaling), anti-phospho-p70 S6K (Thr389; no. 9234; Cell Signaling), anti-phospho-p44/42 mitogen-activated protein kinase (MAPK) (Thr202/Tyr204; no. 9106; Cell Signaling), anti-p44/42 MAPK (no. 9102L; Cell Signaling), anti-phospho-p38 MAPK (Thr180/Tyr182; no. 9211; Cell Signaling), anti-p38 MAPK (no. 9212; Cell Signaling), anti-cytokeratin 8 (no. 10R-C177ax; Fitzgerald), anti-α-smooth muscle actin (no. A2547; Sigma-Aldrich), anti-keratin 5 (no. CLPRB-160P; Covance), anti-E-cadherin (no. 610181; BD Biosciences), anti-N-cadherin (no. 610920; BD Biosciences), and anti-cytokeratin 8 (no. 10R-C177ax; Fitzgerald). The secondary reagents were horseradish peroxidase (HRP)-linked anti-mouse IgG (no. NA931VGE; Healthcare) and HRP-linked protein A (no. NA9120V; GE Healthcare).

Immunofluorescence. Tissues were fixed overnight in 4% paraformaldehyde, embedded in an optimum cutting temperature (OCT) formulation of water-soluble glycols and resins (VWR, Radnor, PA), and frozen. Sections (10 μm) were cut and used in the following procedures. Cells were first cultured on glass coverslips. After reaching 50% confluence, they were fixed for 15 min at room temperature with 4% paraformaldehyde. Frozen tissue sections and cells were permeabilized with 0.5% Triton X-100, in the presence of 10% goat serum diluted in blocking buffer (phosphate-buffered saline [PBS], 5% bovine serum albumin [BSA], 0.02% Tween 20) as the blocking reagent. Samples were then incubated overnight at 4°C with the primary antibodies. The primary antibodies used in this study were anti-Ki67 (no. ab155580; Abcam), anti-cytokeratin 8 (no. 10R-C177ax; Fitzgerald), anti-α-smooth muscle actin (no. A2547; Sigma-Aldrich), and anti-keratin 5 (no. CLPRB-160P; Covance). After incubation for 1 h at room temperature with the secondary antibodies (coupled to Alexa Fluor 647 or Alexa Fluor 488 [Life Technologies]), samples were mounted in mounting medium containing DAPI (4′,6′-diamidino-2-phenylindole; no. H-1200; Vector Laboratories, Burlingame, CA) to detect nuclei.

Immunohistochemistry. Sections of formalin-fixed, paraffin-embedded tissues were rehydrated using xylene and graded alcohols, and antigen retrieval was performed by boiling for 15 min in antigen retrieval buffer (no. H-3300; Vector Laboratories, Burlingame, CA). Samples were then incubated with 3% H_2O_2 for 10 min to quench endogenous peroxidase activity, using 10% goat serum in PBSTT (PBS, 0.02% Tween 20,

0.5% Triton X-100) as the blocking reagent. They were subsequently incubated overnight at 4°C or for 1 h at room temperature with primary antibodies diluted in PBSTT and 1% goat serum. The primary antibodies used were anti-CD3 (no. ab16669; Abcam), anti-CD20 (no. PA5-16701; Thermo Fisher Scientific), anti-F4/80 (no. CL8940AP; Cedarlane), and anti-cleaved caspase-3 (no. 9664; Cell Signaling). Immunoreactive products were detected using biotinylated anti-rat or anti-rabbit IgG (Vector Laboratories), followed by streptavidin-HRP (no. 40525; BD Biosciences). Signals were amplified and visualized using the 3,3′-diaminobenzidine (DAB) HRP substrate kit (no. SK-4100; Vector Laboratories, Burlingame, CA). Sections were also counterstained with hematoxylin, dehydrated, and mounted using Permount solution (Fisher Scientific, Waltham, MA). Negative controls were included for each staining.

Microscopy. For immunofluorescence, samples were analyzed by confocal microscopy using an LSM 710 confocal microscope system (Carl Zeiss, Jena, Germany). Image analysis was carried out using Zen software (Carl Zeiss, Jena, Germany), whereas fluorescence intensity was analyzed using ImageJ software (NIH, Bethesda, MD). For immunohistochemistry, samples were analyzed using an Axiovert S100 TV microscope (Carl Zeiss MicroImaging, Jena, Germany). Images were taken using a digital camera and analyzed with Northern Eclipse software (Empix Imaging, USA). Phase-contrast microscopy was performed using an Axiophot MZ12 microscope (Carl Zeiss MicroImaging, Jena, Germany). Images were taken using a digital camera.

Cell proliferation assays. Cells (2,000 cells in 100 μl of culture medium) were seeded in triplicate in 96-well plates. After various times, 10 μl of the cell proliferation reagent WST1 (Roche, Indianapolis, IN) was added to the culture medium. After 4 h of incubation at 37°C, absorbance was measured at 450 nm using a microplate reader (PowerWave X; Bio-Tek Instruments Inc., Winooski, VT).

Anoikis assays. Cells (50,000 cells per well) were seeded in 24-well ultralow-attachment polystyrene culture dishes (Corning, New York, NY). After 3 days, cells were harvested and resuspended in 75 μl of annexin V buffer containing 1 μl of annexin V (eBioscience, San Diego, CA) and 2.5 μl of propidium iodide (PI; eBioscience, San Diego, CA). After staining in the dark for 15 min, cell suspensions were strained through a 70-μm cell strainer (VWR, Radnor, PA) and subjected to flow cytometry analysis (CyAn ADP; Beckman Coulter, USA). Apoptotic cells were defined as annexin V- and PI-positive cells.

Migration and invasiveness assays. Migration and invasiveness assays were performed using a 24-well Transwell insert (Corning, NY) with a pore size of 8 μm. For migration assays, uncoated inserts were used. For invasiveness assays, inserts were precoated with 100 μl of Matrigel (1:30 dilution; BD Bioscience, San Jose, CA). Cells (10^5 in 100 μl of serum-free medium) were seeded in the upper chamber of the Transwell apparatus, while medium (800 μl) containing 20% fetal bovine serum (FBS) was placed in the lower chamber as chemoattractant. After 24 h, cells on the upper surface of the insert were manually removed with a cotton swab. Cells on the lower surface of the insert membrane were fixed with 4% paraformaldehyde and stained with 0.01% crystal violet in 20% ethanol. Quantification was done by counting the number of cells on the underside of the membrane using a microscope.

Pyk2 inhibition. Tumor-derived cell lines were treated for 3 days with various concentrations of PF431396, a Pyk2 inhibitor (26) (Sigma-Aldrich, Oakville, Canada). Then, cells were processed for immunoprecipitation, immunoblotting, proliferation assays, or Transwell migration assays. Cell viability was confirmed by staining with 7-aminoactinomycin D (7-AAD; eBioscience, San Diego, CA) followed by flow cytometry analysis.

Real-time PCR analyses. Total RNA was extracted from tumor tissues of similar weights or cell lines using an RNeasy kit (Qiagen, Toronto, Canada), according to the manufacturer's instructions. Equal amounts of total RNA (1 μg) were reverse transcribed with random hexamers (SuperScript Vilo cDNA synthesis kit; Invitrogen, New York, NY). Then, real-time PCR analyses were performed using 50 ng of cDNA, the primers specified below, and SYBR green PCR master mix (Applied Biosystems, New York, NY). Reactions were conducted in triplicate using a ViiA 7 real-time PCR system (Applied Biosystems). An annealing temperature of 60°C was used for all reactions. Analysis was performed using ViiA 7 RUO software (Applied Biosystems). Expression levels were normalized using the housekeeping gene *Gapdh*. The $2^{-\Delta\Delta CT}$ method was used to quantify relative changes (*n*-fold). The following oligonucleotides were used for real-time PCR: for *Ptpn12*, 5′ ACAGAGCTGCTGAGTCGTCAGAG 3′ and 5′ ACAGGTGTGGCATTTTCAGGTCC 3′; for *Mmp2*, 5′ CGCTCA GATCCGTGGTGA 3′ and 5′ CGCCAAATAAACCGGTCCTT 3′; for *Snail1*, 5′ TCTGAAGATGCACATCCGAAGCCA 3′ and 5′ AGGAGAAT GGCTTCTCACCAGTGT 3′; for *Snail2*, 5′ AGATGCACATTCGAAC CCAC 3′ and 5′ GTCTGCAGATGAGCCCTCAG 3′; for *E-cadherin*, 5′ GACAACGCTCCTGTCTTCAAC 3′ and 5′ TCTGTGACAACAACGAA CTGC 3′; for *N-cadherin*, 5′ ATTGTCTGATCCTGCCAACTG 3′ and 5′ CAGTGTTCCTGTCCCAC-TCAT 3′; for *Vimentin*, 5′ GTTTCCAAGCC TGACCTCACTG 3′ and 5′ CTCTTCCATCTCACGCATCTGG 3′; for *Zeb1*, 5′ GGAAACCGCAAGTTCAAGTG 3′ and 5′ CACCACACCCTGA GGAGAAC 3′; for *Zeb2*, 5′ AGCTCGAGAGGCATATGGTG 3′ and 5′ TGTTTCTCATTCGGCCATTT 3′; for *Ccnd2*, 5′ GGTGCAGTGTGCAT GTTCCT 3′ and 5′ GCCAGGTTCCACTTCAGCTT 3′; for *TGFβ1i1*, 5′ GCCTCTGTGGCTCCTGCAATAAAC 3′ and 5′ CTTCTCGAAGAAGC TGCTGCCTC 3′; for *Ki67*, 5′ TCAATGTGCCTCGCAGTAAG 3′ and 5′ GCATCTTTGGGGTTTTCTCA 3′; for *SMA*, 5′ ATCGTCCACCGCAA ATGC 3′ and 5′ AAGGAACTGGAGGCGCTG 3′; for *Krt5*, 5′ AAGCTG CTGGAGGGCGAGGAATG 3′ and 5′ CGGGAGGAGGAGGTGGTGG AGAC 3′; for *Krt8*, 5′ GGACATCGAGATCACCACCT 3′ and 5′ TGAA GCCAGGGCTAGTGAGT 3′; and for *GAPDH*, 5′ TGCAGTGGCAAAG TGGAGAT 3′ and 5′ TTTGCCGTGAGTGGAGTCATA 3′.

Statistics. A two-tailed Student's *t* test was used to determine statistical significance. *P* values were calculated using Prism software (GraphPad, La Jolla, CA). A *P* value of less than 0.05 was considered significant. Values presented here are means with standard errors of the means (SEM). Tumor-free survival was determined and compared by the log rank test.

Study approval. Mice were housed in individually ventilated cages in a specific-pathogen-free (SPF) facility. All animal experimentation was approved by the Institut de Recherches Cliniques de Montréal Animal Care Committee and performed in accordance with the regulations of the Canadian Council for Animal Care.

RESULTS

PTPN12 deficiency accelerates tumor development in an ErbB2-dependent mouse model of breast cancer. To help our comprehension of the role of PTPN12 in breast cancer, we took advantage of a well-studied mouse model of ErbB2-dependent breast cancer, termed MMTV-NIC (22, 27). In this model, developed in the mouse strain FVB, a constitutively activated form of ErbB2 is expressed under the control of the mouse mammary tumor virus (MMTV) promoter. This promoter enables expression of activated ErbB2 in mammary epithelial cells, thereby causing breast tumors that are in many ways akin to luminal-type breast cancer in humans (27). The MMTV promoter is also part of a bicistronic construct allowing coexpression of Cre recombinase, which deletes floxed alleles, in cells expressing the activated ErbB2.

The MMTV-NIC mouse was bred with a mouse carrying a floxed allele of *Ptpn12* (*Ptpn12*$^{fl/fl}$) (7), which had been previously backcrossed for at least 20 generations to FVB. Female mice were then monitored for breast tumor development by regular palpation of mammary glands. Both homozygous MMTV-NIC *Ptpn12*$^{fl/fl}$ and heterozygous MMTV-NIC *Ptpn12*$^{fl/+}$ mice were analyzed. MMTV-NIC *Ptpn12*$^{+/+}$ mice served as controls. All animals developed clinically appreciable multifocal breast cancer over time (Fig. 1A and B). All control MMTV-NIC *Ptpn12*$^{+/+}$

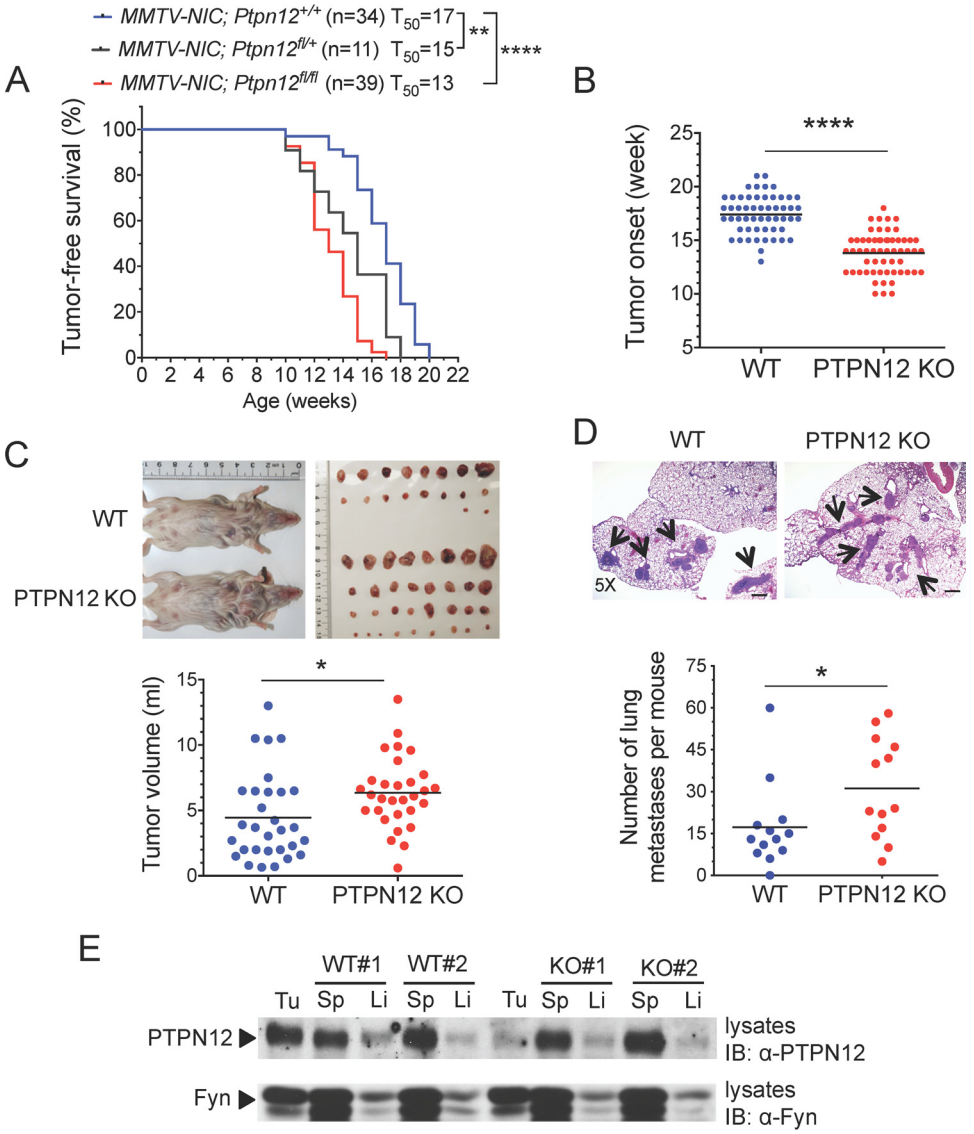

FIG 1 Impact of PTPN12 deficiency on mammary tumor development. (A) Tumor-free incidence was analyzed over time in the indicated groups of mice. The number of mice in each group (n) is indicated. T_{50} represents the age at which 50% of mice had palpable mammary tumors. **, $P = 0.0069$; ****, $P < 0.0001$. (B) Time of onset of tumors in individual mice. Each symbol represents a mouse. WT, wild-type mice (MMTV-NIC *Ptpn12*$^{+/+}$); PTPN12 KO, PTPN12-deficient mice (MMTV-NIC *Ptpn12*$^{fl/fl}$). ****, $P < 0.0001$. (C) Examples of tumors (top) and quantification of tumor volumes (bottom) in individual mice. Each symbol represents a mouse. *, $P = 0.0184$. (D) Representative images of lung sections stained with hematoxylin and eosin (H&E) (top). Arrows depict tumor cell clusters. Bar, 0.5 mm. The graph shows total numbers of lung metastases per mouse (bottom). Symbols represent individual mice. *, $P = 0.0436$. (E) Expression of PTPN12 in spleen (Sp) and liver (Li) was determined by anti-PTPN12 immunoblotting of tissues from two different mice of each genotype (1 and 2). Tumor (tu) tissue from a single mouse of each genotype was analyzed as a control. Fyn was used as a loading control.

mice developed breast cancer by the age of 20 weeks, with an average time to tumor detection of 17 weeks. In comparison, homozygous MMTV-NIC *Ptpn12*$^{fl/fl}$ mice developed breast cancer significantly faster. All mice displayed breast tumors by the age of 17 weeks, and average time to tumor appearance was 13 weeks. As tumors develop rapidly in this mouse model, this ~4-week difference is remarkable. Tumors from PTPN12-deficient mice were also larger and more numerous (Fig. 1C). Heterozygous MMTV-NIC *Ptpn12*$^{fl/+}$ mice had an intermediate phenotype (Fig. 1A and B).

To examine if PTPN12 deficiency also influenced metastases, serial sections were performed on lungs of tumor-bearing mice and stained with hematoxylin and eosin (H&E), 5 weeks after detection of primary tumors, that is, at a younger age for PTPN12-deficient animals (Fig. 1D). In comparison to control mice, mice lacking PTPN12 displayed an ~2.0-fold increase in the number of lung metastases. In keeping with the specificity of the MMTV promoter, MMTV-NIC *Ptpn12*$^{fl/fl}$ mice exhibited loss of PTPN12 expression in breast tumor tissue but not in other tissues, such as spleen and liver (Fig. 1E; also data not shown).

Thus, loss of PTPN12 in breast epithelial cells resulted in accelerated primary tumor development and more frequent metastases in an ErbB2-dependent model of breast cancer.

Primary breast tumors and tumor-derived cell lines lacking PTPN12 exhibit minimally altered histology. Microscopic anal-

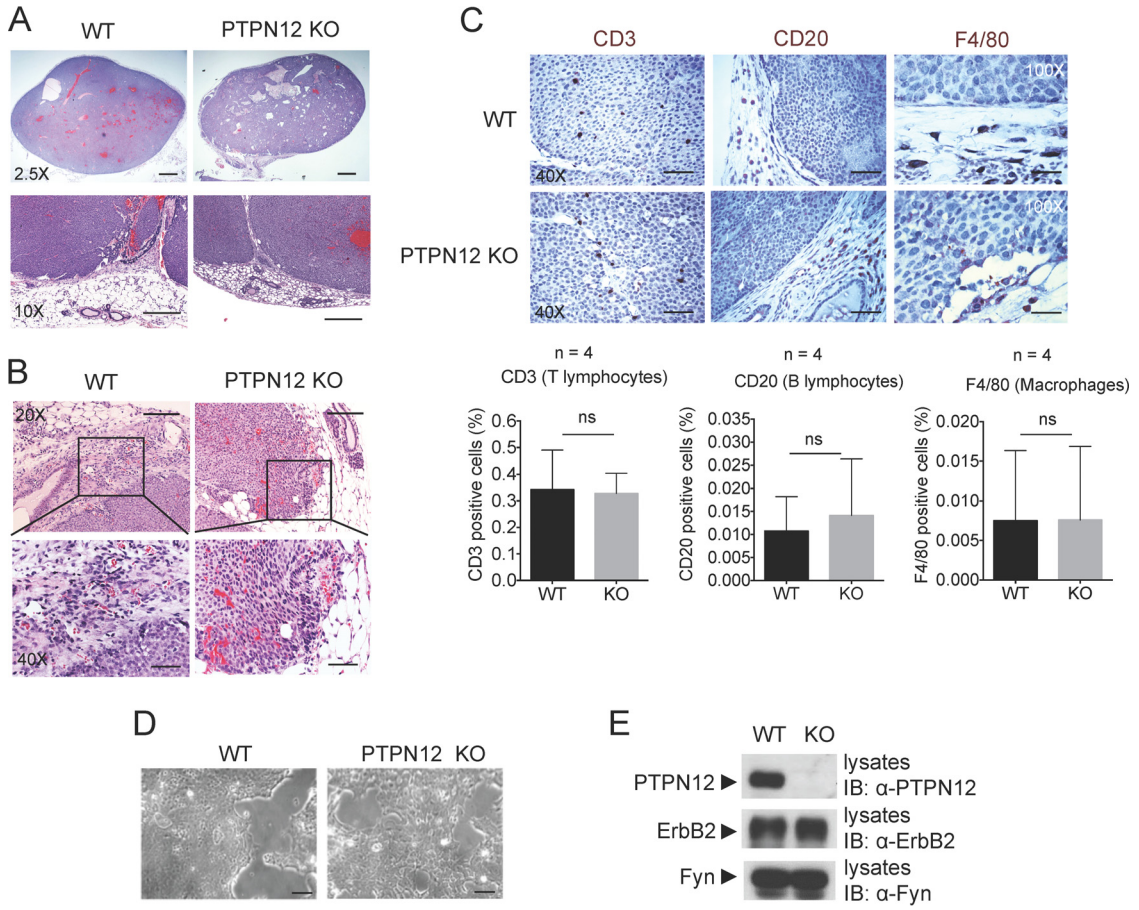

FIG 2 Morphological analyses of PTPN12-deficient tumors and cell lines. (A and B) Primary tumors were stained with H&E and analyzed by microscopy at the indicated magnifications. Representative images are shown. Bars, 0.5 mm (A, top), 0.3 mm (A, bottom), 125 μm (B, top), and 60 μm (B, bottom). WT, wild-type mice (MMTV-NIC *Ptpn12*$^{+/+}$); PTPN12 KO, PTPN12-deficient mice (MMTV-NIC *Ptpn12*$^{fl/fl}$). (C) Immunohistochemistry was performed to identify infiltration of primary tumors with T cells (anti-CD3), B cells (anti-CD20), and macrophages (F4/80). Representative images are shown. Bars, 60 μm (CD3 and CD20) and 25 μm (F4/80). The graph shows data from multiple mice (the number of mice [n] is given). Positive cells were counted using ImageJ. The percentages of positive cells from 16 different fields of 4 tumors per genotype were quantified. Average values with standard deviations are shown. *P* values were 0.8832 (CD3), 0.408 (CD20), and 0.9866 (F4/80). (D) Morphological appearance of tumor-derived cell lines from the indicated mice was analyzed by microscopy. Representative cell lines are shown. Bars, 60 μm. (E) Expression of PTPN12 in representative tumor-derived cell lines was determined by immunoblotting. Data are representative of three independent experiments with eight cell lines of each genotype.

yses of H&E-stained sections of primary breast tumors showed no remarkable difference between control and PTPN12-deficient mice (Fig. 2A and B). Tumors from either mice exhibited a nodular appearance with large sheets of monomorphous cells and areas of necrosis. There was also no significant difference in the number or the type of immune cells infiltrating the tumors, including T lymphocytes, B lymphocytes, and macrophages (Fig. 2C).

Breast tumor tissue contains not only transformed epithelial cells but also stromal cells and immune cells. Therefore, to help clarify the impact of PTPN12 deficiency, primary epithelial cell lines were derived from breast tumors that did or did not express PTPN12. To ensure reproducibility of our findings, multiple cell lines were generated from multiple mice. Both in control and in PTPN12-deficient mice, cell lines had an epithelium-like morphology (Fig. 2D). No significant difference in morphology was noted. Immunoblot analyses confirmed that cells from control mice expressed PTPN12, whereas those from *Ptpn12*$^{fl/fl}$ mice did not (Fig. 2E). Both still expressed ErbB2. They also had equal levels of Fyn, the expression of which is not affected by PTPN12 deficiency and which was used as loading control.

Hence, lack of PTPN12 did not provoke any obvious alteration in the histological appearance of primary tumors or tumor-derived cell lines.

Breast cancer cells lacking PTPN12 display enhanced tyrosine phosphorylation of Cas, Pyk2, and paxillin but not ErbB2, FAK, and Shc. To identify the targets of PTPN12 in breast cancer, the tyrosine phosphorylation substrates hyperphosphorylated in cell lines lacking PTPN12 were detected by immunoblotting of total cell lysates with antiphosphotyrosine antibodies (Fig. 3A). In contrast to cells expressing PTPN12, cells devoid of PTPN12 displayed prominently augmented tyrosine phosphorylation of one or more proteins migrating at ~120 to 130 kDa. Other substrates, including polypeptides of 90, 70, and 55 kDa, were less reproducibly affected. This difference was seen in multiple independent cell lines.

Known phosphotyrosine-containing targets of PTPN12 or ErbB2 were immunoprecipitated with specific antibodies and

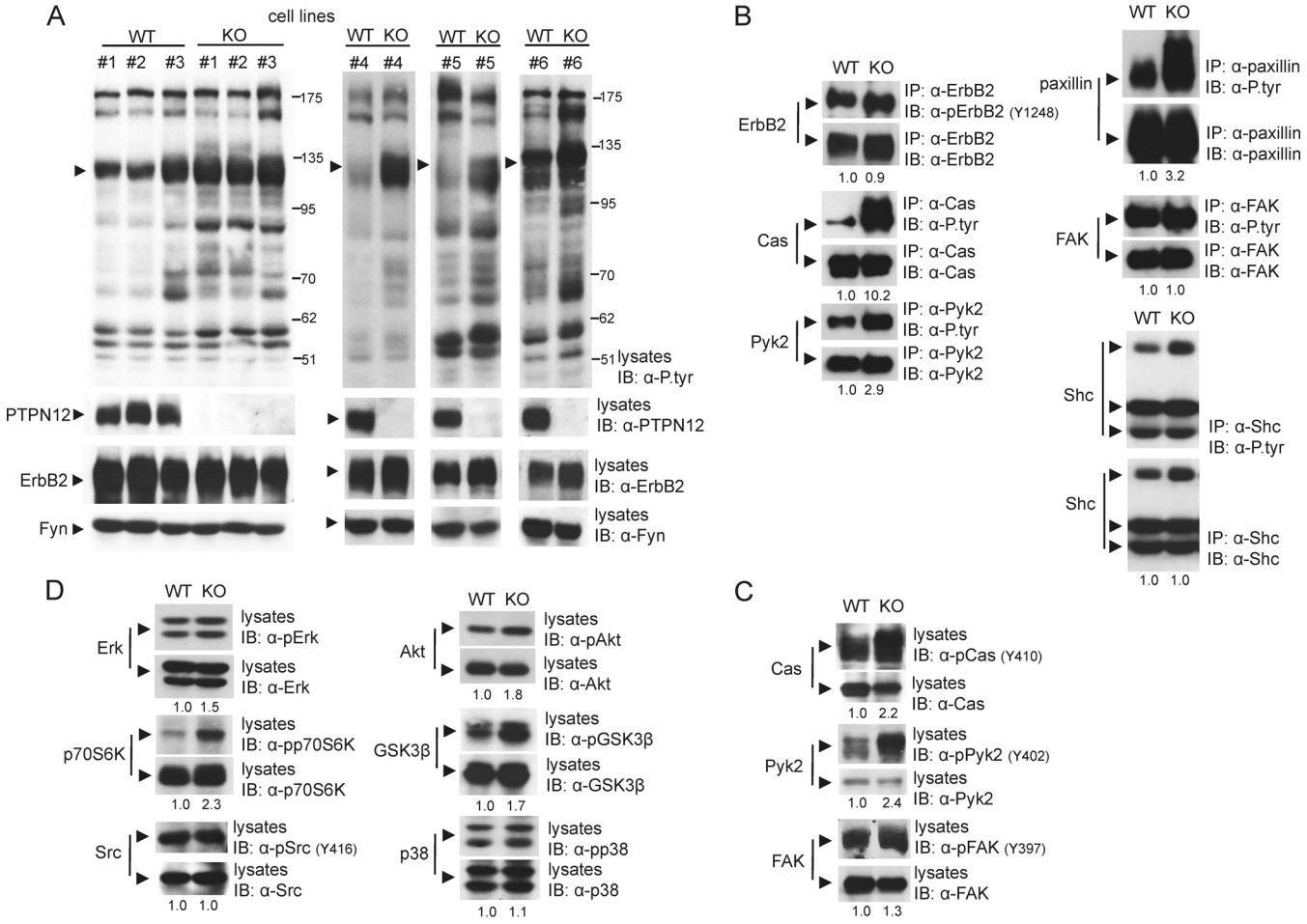

FIG 3 Biochemical impact of PTPN12 deficiency in tumor-derived cell lines. The impact of PTPN12 on protein tyrosine phosphorylation and downstream kinase activation was examined using tumor-derived cell lines. Representative data are depicted. WT, wild-type mice (MMTV-NIC *Ptpn12*$^{+/+}$); PTPN12 KO, PTPN12-deficient mice (MMTV-NIC *Ptpn12*$^{fl/fl}$). (A) Overall protein tyrosine phosphorylation was determined by immunoblotting of total cell lysates with antiphosphotyrosine (P.tyr) antibodies. The positions of the dominant polypeptides displaying enhanced tyrosine phosphorylation are shown on the left, while those of prestained molecular mass markers are on the right. Lysates from six cell lines of each genotype were analyzed. (B) Tyrosine phosphorylation of the indicated substrates was ascertained by immunoprecipitation with substrate-specific antibodies, followed by antiphosphotyrosine immunoblotting. Reprobing of the immunoblot membranes confirmed equal expression levels of the indicated proteins. Quantitation of relative protein tyrosine phosphorylation is shown at the bottom. (C) As for panel B, except that tyrosine phosphorylation of the indicated substrates was assessed by immunoblotting of total cell lysates with phospho-specific antibodies. (D) As for panel B, except that activation of the indicated downstream kinases was assessed by immunoblotting of total cell lysates with phospho-specific antibodies. Data are representative of at least three independent experiments with five cell lines of each genotype.

probed by antiphosphotyrosine immunoblotting (Fig. 3B). Tyrosine phosphorylation of the adaptor Cas, the PTK Pyk2, and the adaptor paxillin was augmented in cells lacking PTPN12, in comparison to control cells. In contrast, there was no difference in the phosphotyrosine content of ErbB2, FAK, and Shc. These results were confirmed by immunoblotting of total cell lysates with phosphospecific antibodies available against some of these targets (Fig. 3C). There was no augmentation of the extent of tyrosine phosphorylation of Src, a known effector of transformation in the ErbB2-driven mouse breast cancer model (28). Immunoblotting with phospho-specific antibodies showed small increases in the activity of GSK3β and p70S6 kinase but not of Erk, Akt, and p38 (Fig. 3D).

To ensure that these changes were due to PTPN12 deficiency rather than clonal variation, PTPN12 was reintroduced in PTPN12-deficient cells, by infection with a green fluorescent protein (GFP)-based retroviral vector and subsequent cell sorting (Fig. 4). Cells expressing GFP alone were produced as controls. Moreover, cells from mice expressing PTPN12 were infected in parallel. After cell sorting, ~40% and ~80% of cells infected with PTPN12-encoding-retroviruses and with GFP-encoding retroviruses were GFP positive, respectively (Fig. 4A). These findings suggested that retroviral transduction was not very efficient or stable, especially if the retroviruses encoded PTPN12. Nonetheless, introduction of PTPN12 in PTPN12-deficient cells resulted in appreciable suppression of overall protein tyrosine phosphorylation, as well as of tyrosine phosphorylation of Cas and Pyk2 (Fig. 4B). A small decrease in tyrosine phosphorylation was also seen in cells from PTPN12-expressing mice.

We also examined protein tyrosine phosphorylation in primary breast tumors (Fig. 5). Compared to tumors from control mice, tumors from mice lacking PTPN12 demonstrated augmented tyrosine phosphorylation of polypeptides migrating at 130 kDa (Fig. 5A). Immunoblotting with phospho-specific antibodies revealed hyperphosphorylation of Cas and Pyk2 but not ErbB2 (Fig. 5). This is shown for

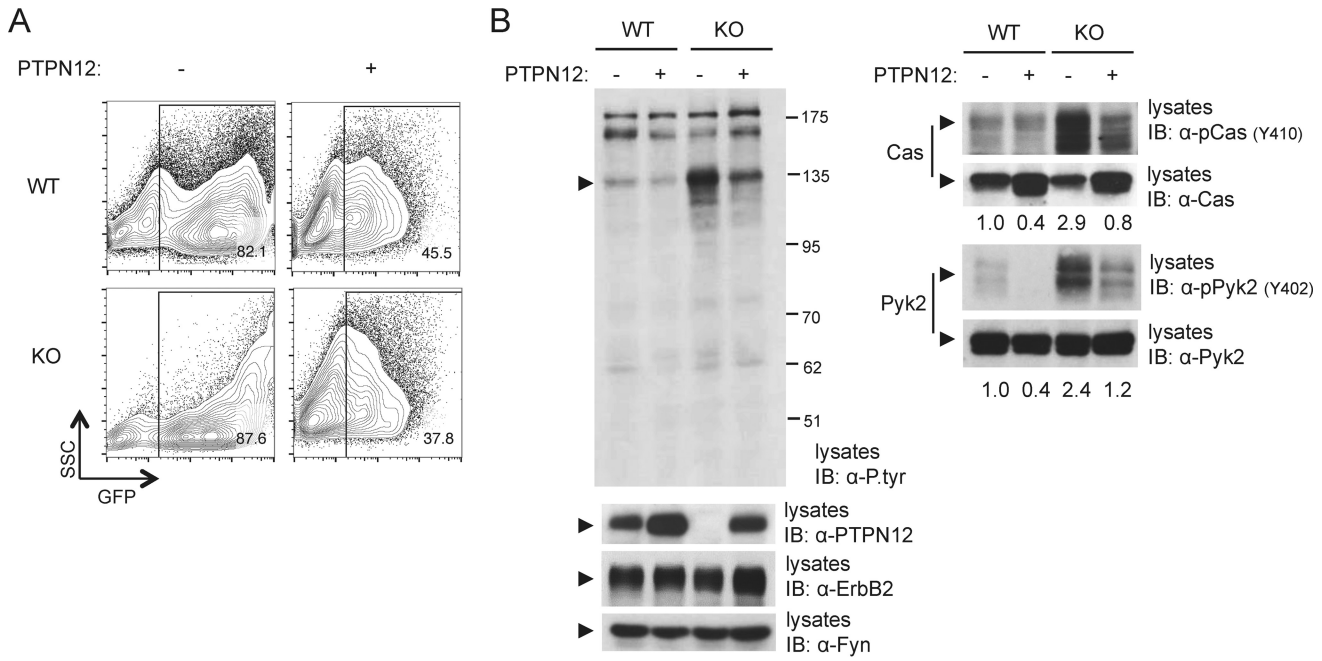

FIG 4 Reexpression of PTPN12 in PTPN12-deficient breast cancer cells. PTPN12 was expressed in wild-type (WT) or PTPN12-deficient (KO) tumor cell lines, using a green fluorescent protein (GFP)-encoding retroviral vector and sorting for GFP-positive cells. Cells expressing GFP alone (−) were generated as controls. (A) After sorting, infected cells were detected by flow cytometry. The percent GFP-positive cells is shown in the right bottom corner. SSC, side scatter. (B) Overall protein tyrosine phosphorylation (left) and tyrosine phosphorylation of Cas and Pyk2 (right) were determined as outlined for Fig. 3A and C, respectively. Quantitation of relative phosphorylation is shown at the bottom. Data are representative of three independent experiments using three different tumor-derived cell lines.

6 different tumors of each genotype. There was no increase in tyrosine phosphorylation of Shc. Of note, protein tyrosine phosphorylation was quite variable between tumors of the same genotype, presumably reflecting tumor heterogeneity.

Therefore, lack of PTPN12 in ErbB2-driven breast cancer cells resulted in hyperphosphorylation of Cas, Pyk2, and paxillin but not FAK, ErbB2, Shc, or Src. It also induced modestly elevated activity of GSK3β and p70S6 kinase. These changes

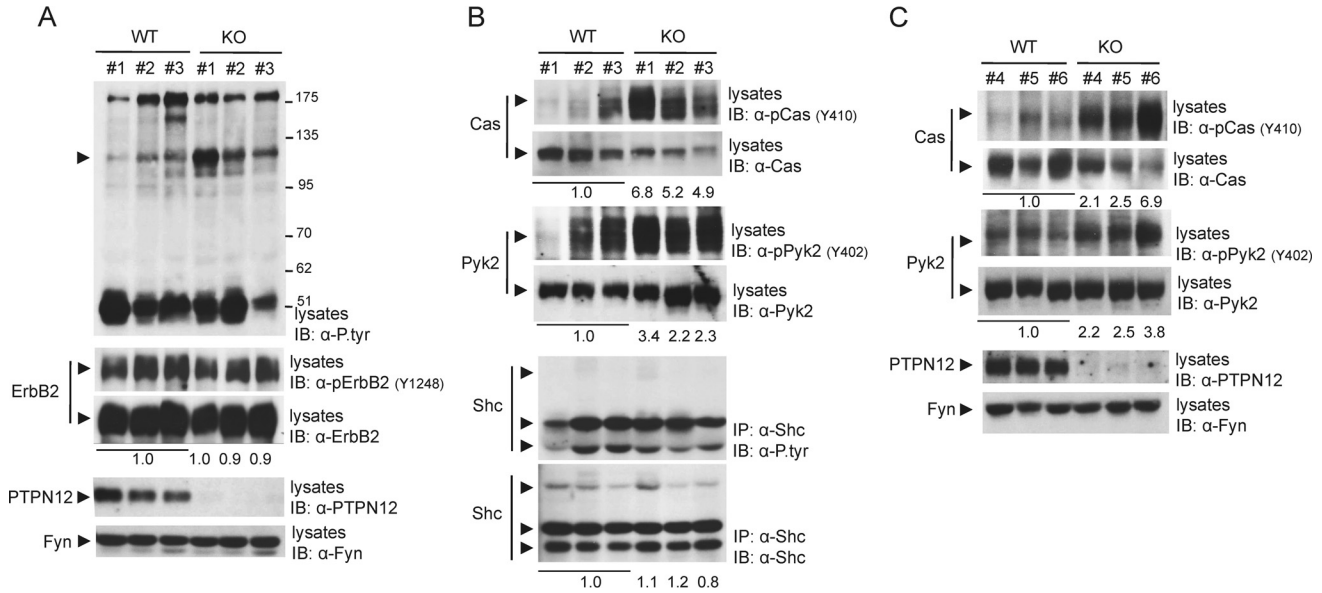

FIG 5 Biochemical impact of PTPN12 deficiency in primary breast tumors. (A) The impact of PTPN12 on protein tyrosine phosphorylation was examined using three independent primary tumors of each genotype. The position of the dominant polypeptide displaying enhanced tyrosine phosphorylation is shown on the left, while those of prestained molecular mass markers are on the right. ErbB2 phosphorylation was assessed by immunoblotting using phospho-specific antibody. WT, wild-type mice (MMTV-NIC *Ptpn12*$^{+/+}$); PTPN12 KO, PTPN12-deficient mice (MMTV-NIC *Ptpn12*$^{fl/fl}$). (B and C) Tyrosine phosphorylation of the indicated substrates was assessed by immunoblotting of total cell lysates with phospho-specific antibodies (Cas and Pyk2), or immunoprecipitation with substrate-specific antibodies followed by antiphosphotyrosine (P.tyr) immunoblotting (Shc). Two different experiments with a total of six tumors of each genotype were analyzed. Quantitation of relative protein tyrosine phosphorylation is shown at the bottom.

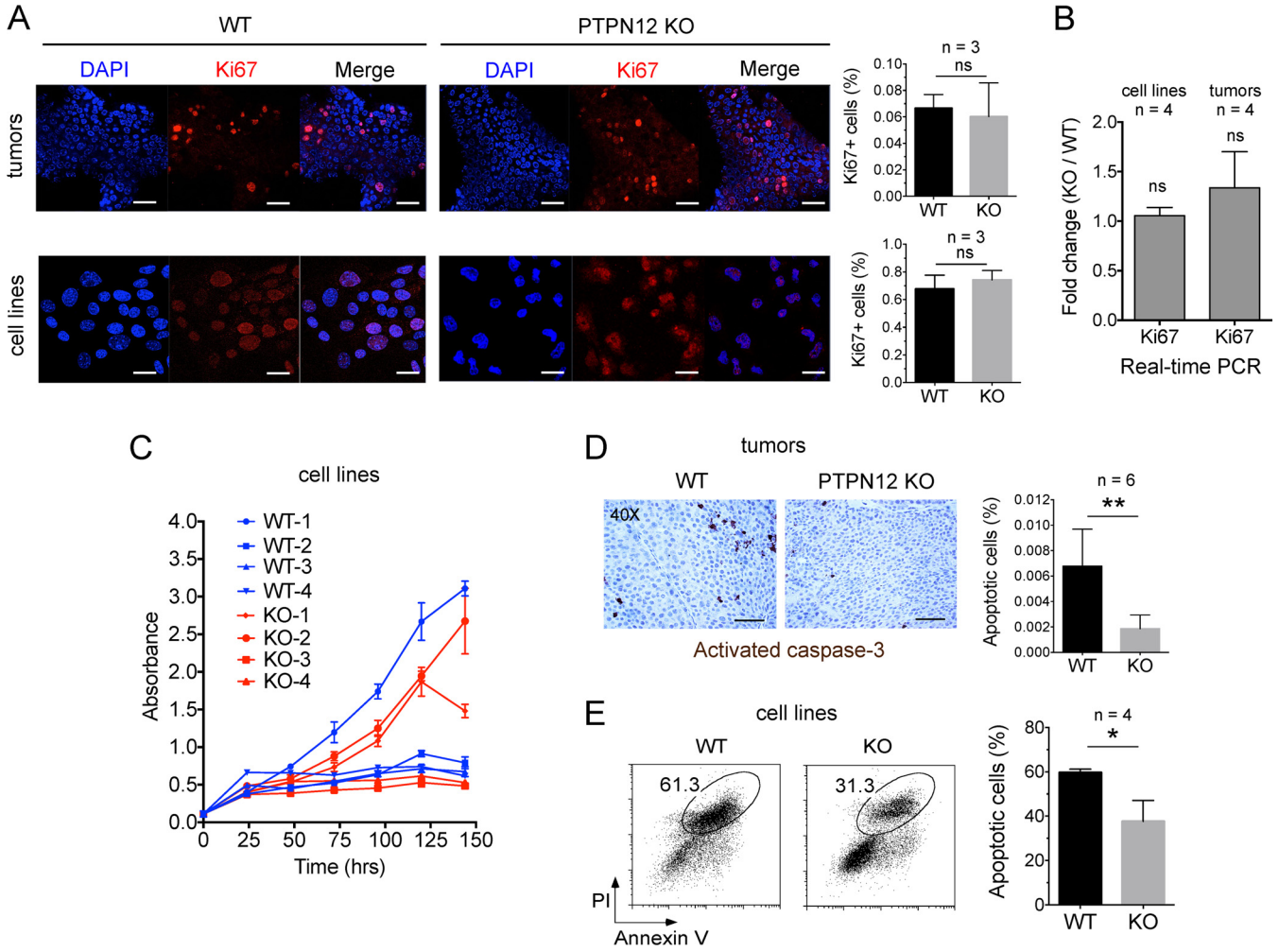

FIG 6 Impact of PTPN12 deficiency on breast cancer cell proliferation and survival. (A) Expression of Ki67 in primary tumors (top) or tumor-derived cell lines (bottom) was analyzed by immunofluorescence. Staining of representative samples with DAPI, which marks nuclei, and a merged image are shown. Bars, 25 μm. The graphs show mean fluorescence intensity in 10 different fields from 3 tumor samples per genotype, with standard deviations. ns, not significant (for tumor tissues, $P = 0.4986$; for cell lines, $P = 0.7062$). WT, wild-type mice (MMTV-NIC *Ptpn12*$^{+/+}$); PTPN12 KO, PTPN12-deficient mice (MMTV-NIC *Ptpn12*$^{fl/fl}$). (B) Quantitative real-time PCR analysis of Ki67 expression in tumor-derived cell lines or primary tumor tissues. RNA samples from four epithelial cell lines or tumor tissues of each genotype were analyzed for quantitative PCR. Ratios of relative expression in KO compared to WT are depicted. Average values with standard deviations are shown. (C) Proliferation of multiple tumor-derived cell lines over 6 days was analyzed using the cell proliferation dye WST1. Absorbance at 450 nm was measured. Average values from triplicates with standard deviations are shown. (D) Activated (cleaved) caspase 3 was measured in primary tumors using immunohistochemistry. Representative samples are shown on the left. Bars, 60 μm. Percentages of cells positive for activated caspase 3 in 25 fields of six tumor samples per genotype are depicted on the right. Average values with standard deviations are shown. **, $P = 0.0032$. (E) Susceptibility of tumor-derived cell lines to anoikis was determined by staining with annexin V and propidium iodide (PI) and flow cytometry. Representative samples are shown on the left. Annexin V- and PI-positive cells (circled, with percentages) correspond to apoptotic cells. The bar graph shows data for four independent cell lines of each genotype. Values are averages from 3 independent experiments, with standard deviations. *, $P = 0.0161$.

were seen both in tumor-derived cell lines and in primary tumors.

PTPN12-deficient breast cancer cells display unaltered proliferation but enhanced survival. To understand how loss of PTPN12 resulted in earlier development of breast cancer, the impact on cell proliferation and survival was examined, using both primary tumor tissues and cell lines (Fig. 6). Control and PTPN12-deficient tumors or cell lines showed no difference in expression of Ki67, a proliferation marker (Fig. 6A). Similar results were obtained by real-time PCR of RNA (Fig. 6B). Likewise, there was no consistent difference in cell proliferation between the two types of tumor-derived cell lines *in vitro*, although there was generally a marked variation in proliferation rates (Fig. 6C).

To test the possibility that loss of PTPN12 promoted cell survival, tumor tissues were stained with antibodies recognizing activated (or cleaved) caspase 3, a marker of apoptosis (Fig. 6D). Tumors derived from PTPN12-deficient mice displayed a marked diminution in the proportion of activated caspase 3-positive cells, in comparison to tumors from control mice. We also tested the susceptibility of tumor cell lines to anoikis, a form of apoptosis triggered by detachment of anchorage-dependent cells from the extracellular matrix (29) (Fig. 6E). To this end, cell lines were trypsinized, and plated in ultralow-attachment culture dishes containing serum-free medium. Apoptotic cells were detected by staining with annexin V and propidium iodide (PI). Compared to control cells, cells from PTPN12-deficient mice showed a reduc-

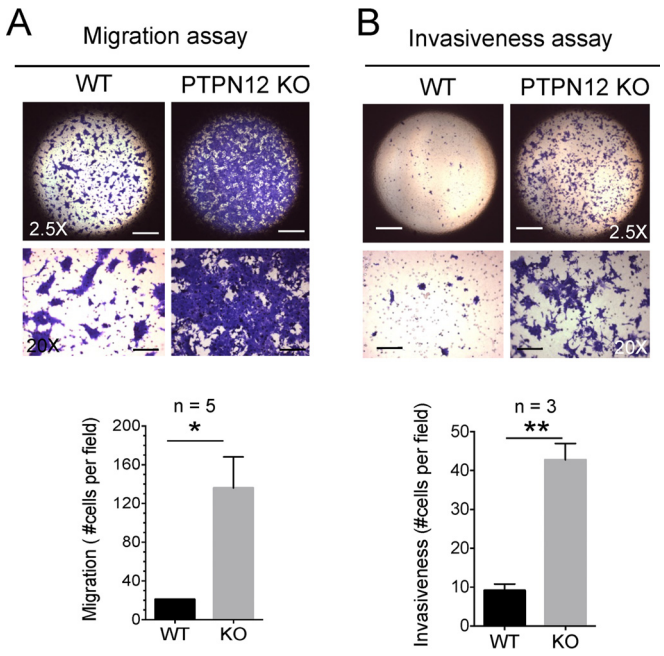

FIG 7 Migration and invasiveness of PTPN12-deficient breast cancer cells. (A) Migration of tumor-derived cell lines was determined using a Transwell migration assay. Cells were placed in the upper chamber, while serum was added to the lower chamber as chemoattractant. After 24 h, migration was quantitated by staining cells on the lower surface of the insert membrane. Representative images are shown. Bars, 0.5 mm (top) and 100 μm (bottom). The graph shows data from multiple independent cell lines. Values are averages with standard deviations. *, $P = 0.0368$. WT, wild-type mice (*MMTV-NIC Ptpn12*$^{+/+}$); PTPN12 KO, PTPN12-deficient mice (MMTV-NIC *Ptpn12*$^{fl/fl}$). (B) Invasiveness was measured as for panel A, except that the insert membrane was precoated with Matrigel. **, $P = 0.0091$. All panels are representative of at least three independent experiments.

tion of annexin V- and PI-positive cells, implying that they underwent reduced anoikis.

Thus, lack of PTPN12 in breast cancer cells had no appreciable impact on cell proliferation but prevented activation of caspase 3 *in vivo* and anoikis *in vitro*.

PTPN12-deficient breast cancer cells have enhanced migration and invasiveness. The increased frequency of lung metastases in PTPN12-deficient animals raised the possibility that migration, invasiveness, or both were enhanced by loss of PTPN12. However, previous studies in various nontransformed cell types demonstrated that PTPN12 was a positive regulator, rather than an inhibitor, of cell migration. But it was plausible that the situation was different for transformed cells. To address this possibility, Transwell migration assays were performed (Fig. 7). In the first assay aimed at analyzing migration, tumor cells were loaded in the upper chamber of a Transwell apparatus, and serum was placed in the lower chamber as a chemoattractant (Fig. 7A). Migration of cells through the porous membrane of the apparatus was then quantitated. In comparison with control cell lines, tumor cells devoid of PTPN12 had markedly increased migration across the membrane.

To ascertain the impact of PTPN12 deficiency on the invasive potential of breast cancer cells, similar experiments were performed using a Transwell apparatus in which the porous membrane was precoated with Matrigel, which contains a mixture of laminin, collagen, and heparan sulfate proteoglycans (Fig. 7B). Invasion of tumor cells from the upper chamber into the membrane was then evaluated. These analyses indicated that the ability of breast cancer cells to invade the Matrigel-coated filter was augmented by PTPN12 deficiency.

Together, these findings indicated that loss of PTPN12 in breast cancer cells increased cell migration and invasiveness. This is in striking contrast to normal cells, in which loss of PTPN12 typically results in reduced migration (5–11).

Evidence for a critical role of Pyk2 in enhanced migration of PTPN12-deficient breast cancer cells. Pyk2 is a cytoplasmic PTK promoting cell migration, at least in part by phosphorylating paxillin (30). Given that loss of PTPN12 resulted in augmented tyrosine phosphorylation of Pyk2 and paxillin, we examined if Pyk2 was implicated in the altered migration properties of PTPN12-deficient cells (Fig. 8). For this purpose, cell lines from PTPN12-deficient mice were briefly treated with a pharmacological inhibitor of Pyk2, PF431396 (26). This inhibitor is known to inactivate Pyk2 and FAK but not Src family kinases. PF431396 caused a dose-dependent inhibition of the extent of tyrosine phosphorylation of Pyk2 and its substrate, paxillin (Fig. 8A). No effect on Src was seen. Importantly, it also triggered a dose-dependent reduction of cell migration in the Transwell migration assay (Fig. 8B). No effect on cell viability was seen (Fig. 8C). However, the inhibitor also caused an inhibition of cell proliferation (Fig. 8D).

These data implied that Pyk2 and, possibly, paxillin played a pivotal role in the augmented migratory properties of PTPN12-deficient breast cancer cells.

Loss of PTPN12 increases expression of markers of basal-type breast cancer and epithelial-to-mesenchymal transition. The MMTV-NIC mouse model has many properties of luminal-type breast cancer, a less aggressive form of breast cancer in humans (27, 31, 32). It has only limited features of the more aggressive basal-type breast cancer. To analyze if loss of PTPN12 had an impact on one or the other subtype of breast cancer, expression of various markers linked to these subtypes was analyzed (Fig. 9). First, immunoblot analyses were performed using lysates from multiple tumor-derived cell lines of control or PTPN12-deficient mice (Fig. 9A; also data not shown). Compared to cells from control mice, cells from mice lacking PTPN12 often exhibited increased expression of smooth muscle actin (SMA) and keratin 5, two markers of basal-type cancer (25, 26). In contrast, they frequently had decreased expression of keratin 8, a marker of luminal-type cancer. As noted earlier for protein tyrosine phosphorylation, there was marked variation between cell lines of the same genotype, whether from control mice or from PTPN12-deficient mice. This likely reflected tumor heterogeneity. Moreover, the differences were not absolute, i.e., control and PTPN12-deficient cells often expressed markers of both subtypes, albeit in different relative amounts. Similar analyses were also performed on primary tumors, using immunoblot analyses (Fig. 9B), real-time PCR (Fig. 9C), or immunofluorescence (Fig. 9D). In all assays, expression of SMA and keratin 5 was enhanced in PTPN12-deficient tumors. Moreover, expression of keratin 8 was diminished, although this effect did not reach statistical significance in the real-time PCR assay.

Aggressive breast cancer is also typically associated with features of EMT, a process in which epithelial cells reduce their polarity and ability to adhere, thereby becoming more migratory and invasive (33, 34). This transformation contributes to the more

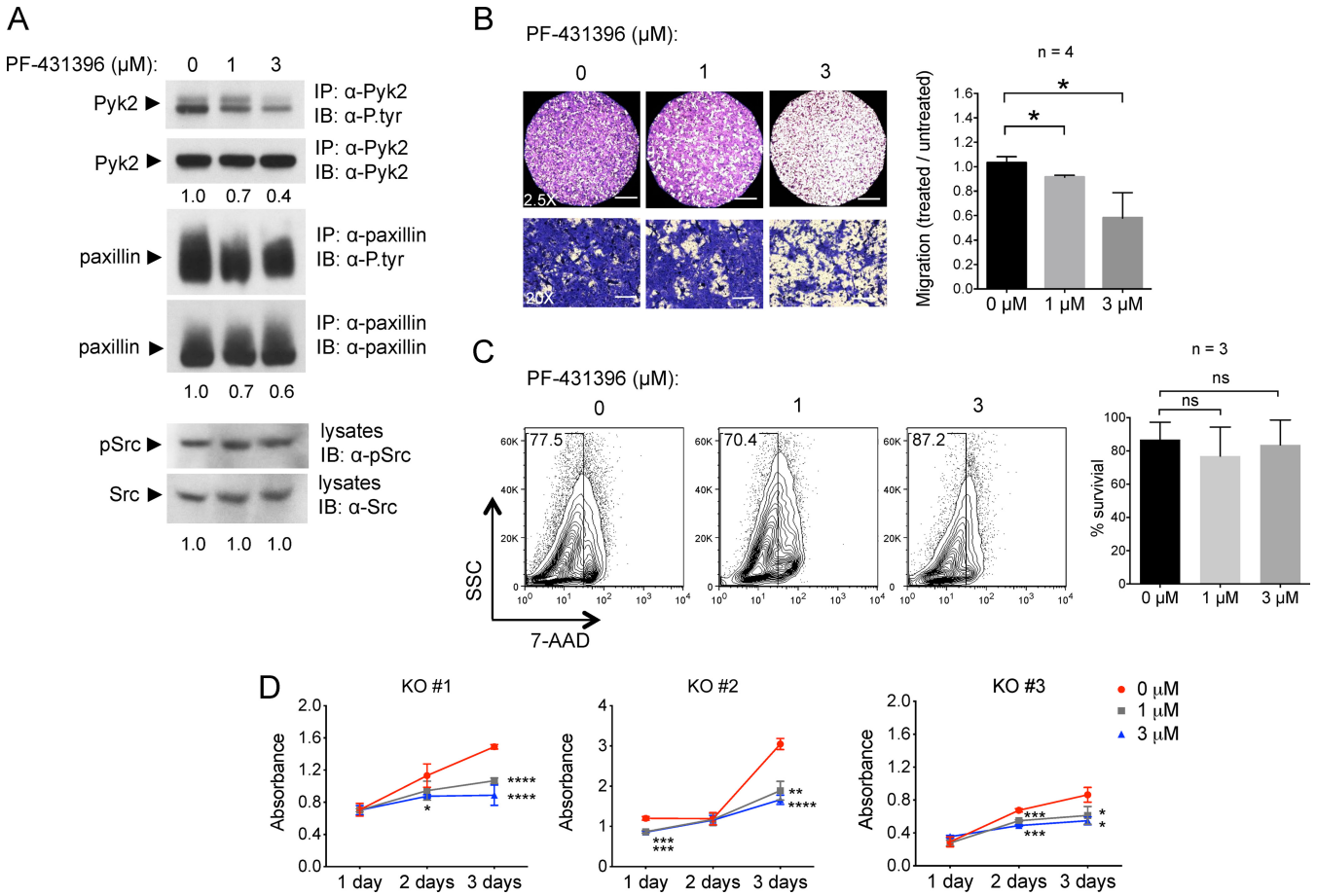

FIG 8 Impact of Pyk2 inhibition on PTPN12-deficient tumor cells. PTPN12-deficient tumor-derived cells were treated for 3 days with the indicated concentrations of PF431396, a Pyk2 inhibitor, or left untreated. (A) Tyrosine phosphorylation of the indicated substrates was ascertained by immunoprecipitation with substrate-specific antibodies, followed by antiphosphotyrosine (P.tyr) immunoblotting. c-Src phosphorylation at the activating tyrosine, tyrosine 416, was determined by immunoblotting with a phospho-specific antibody. Reprobing of the immunoblot membranes confirmed equal expression levels of the indicated proteins. Quantitation of relative protein tyrosine phosphorylation is shown at the bottom. (B) Migration was assessed as described for Fig. 7A. Representative images are shown. The graph shows ratios of migration in treated cells to that in untreated cells in multiple independent experiments. Values are averages with standard deviations. Data are representative of four independent experiments with four cell lines. *, $P = 0.0139$ (1 μM versus 0 μM) and 0.0167 (3 μM versus 0 μM). (C) Survival of cells treated with the indicated concentrations of Pyk2 inhibitor was measured by staining with 7-AAD and detection of stained cells by flow cytometry. Representative images are shown. The percent viable cells is shown at the top left of each scatter plot. SSC, side scatter. The bar graph shows average survival with standard deviations for three cell lines in three independent experiments. ns, not significant. (D) Proliferation of cells treated with the indicated concentrations of Pyk2 inhibitor was analyzed as detailed for Fig. 6C. *, $P < 0.05$; **, $P < 0.01$; ***, $P < 0.001$; ****, $P < 0.0001$.

invasive and aggressive behavior of basal-type breast cancer, in comparison to luminal-type breast cancer. To ascertain if loss of PTPN12 promoted EMT, expression of EMT markers was examined using real-time PCR (Fig. 10A). Compared to control cell lines, cell lines from PTPN12-deficient tumors had statistically significant increases in levels of RNAs encoding several EMT markers, including the EMT transcription factors Zeb1 and Zeb2, N-cadherin (*Cdh2*), cyclin D2 (*Ccdn2*), and matrix metalloprotease 2 (MMP-2) (*Mmp2*) (34). Paradoxically, there was little or no alteration of E-cadherin (*Cdh1*), an epithelial marker. The change in expression of N-cadherin but not E-cadherin was confirmed by immunoblotting of total cell lysates with the relevant antibodies (Fig. 10B). Similar analyses were performed on primary breast tumors (Fig. 10C and D). Tumors from PTPN12-deficient mice also showed increased RNA expression for several EMT markers, in comparison to tumors from control mice (Fig. 10C). They also had increased expression of N-cadherin at the protein level (Fig. 10D).

Thus, lack of PTPN12 in ErbB2-induced breast cancer promoted partial acquisition of markers of basal-type breast cancer and EMT. This was accompanied by a partial loss of markers of luminal-type breast cancer.

DISCUSSION

The results presented herein showed that loss of PTPN12 in breast epithelial cells resulted in significant acceleration of breast cancer development in a mouse model of ErbB2-dependent breast cancer, MMTV-NIC. PTPN12-deficient animals developed detectable breast tumors ~4 weeks earlier than PTPN12-expressing mice. Their tumors were also larger and more numerous. They were associated with a greater frequency of lung metastases. Heterozygous PTPN12-deficient mice had a phenotype intermediate between those of PTPN12-expressing and homozygous PTPN12-deficient mice, implying that the tumor-suppressing effect of PTPN12 was dose dependent. Thus, as suggested for hu-

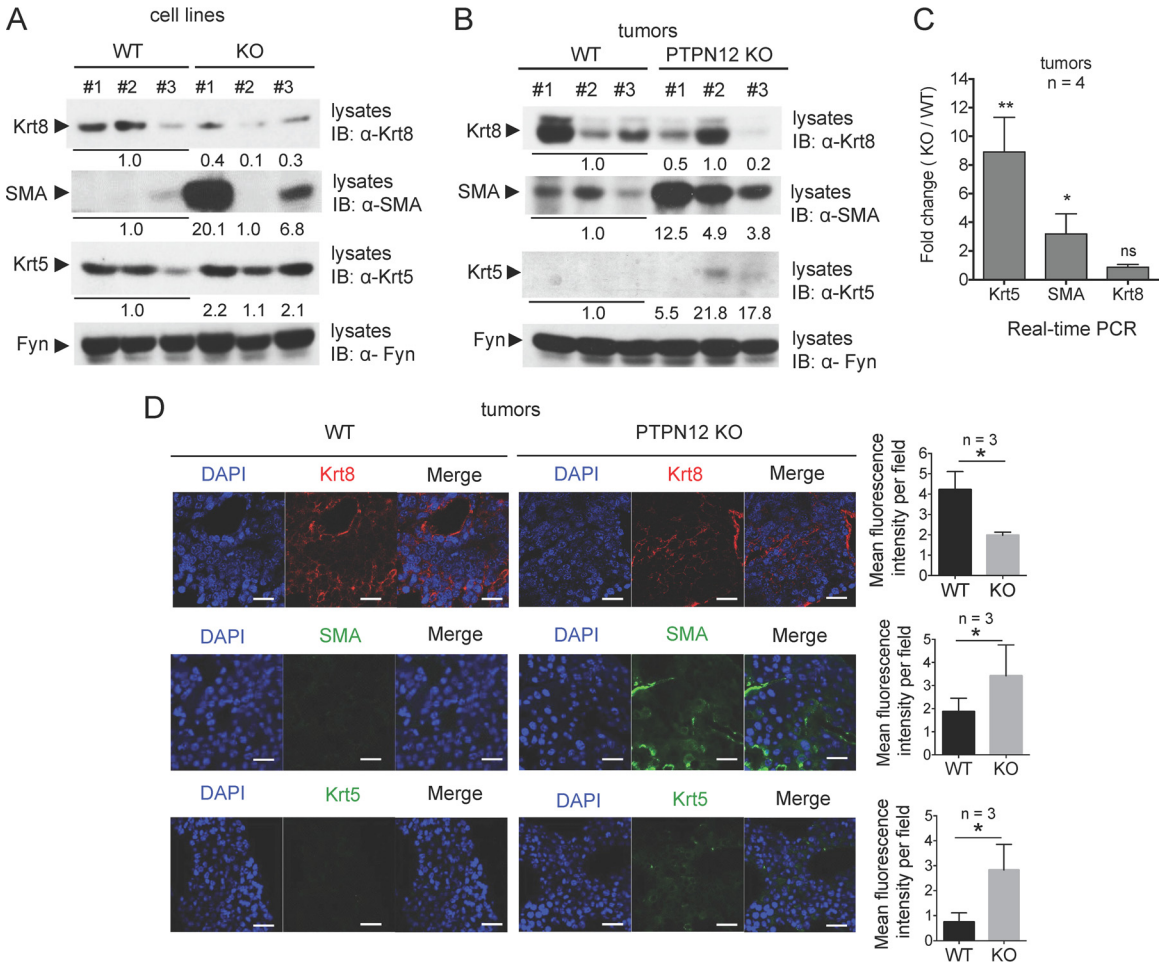

FIG 9 Altered expression of basal-type and luminal-type markers in PTPN12-deficient breast tumors and cell lines. (A and B) Lysates from tumor-derived cell lines (A) or primary breast tumors (B) were analyzed by immunoblotting with the indicated antibodies. (A) Data from representative cell lines; (B) data from three independent primary tumors. Krt8, keratin 8; SMA, smooth muscle actin; Krt5, keratin 5; WT, wild-type mice (MMTV-NIC *Ptpn12*$^{+/+}$); PTPN12 KO, PTPN12-deficient mice (MMTV-NIC *Ptpn12*$^{fl/fl}$). Quantitation of relative protein expression is shown at the bottom. (C) RNA samples from 4 tumor tissues of each genotype were analyzed for real-time PCR. Ratios of relative expression in KO compared to WT are depicted. Average values with standard deviations are shown. **, $P < 0.01$; *, $P < 0.05$. (D) Expression of the indicated markers in primary tumors was analyzed by immunofluorescence. Staining with DAPI, which marks nuclei, and a merged image of representative samples are shown. Bars, 25 μm. The graphs show mean fluorescence intensities in 10 different fields, determined by average optical density (AOD). Values are averages for 3 tumor samples per genotype, with standard deviations. *, $P = 0.0125$ (Krt8), 0.0106 (SMA), and 0.0299 (Krt5). All panels are representative of at least 3 experiments.

man breast cancer (14, 16, 17), PTPN12 is a suppressor of breast cancer development and progression in the MMTV-NIC model.

Histological analyses of primary breast tumors showed that PTPN12 deficiency had no appreciable impact on the morphological appearance of tumors. It also had no effect on the infiltration of tumors by T cells, B cells, and macrophages, which are known to influence tumor progression. Likewise, cell lines established from primary tumors of PTPN12-deficient mice displayed an unaltered epithelial morphology compared to cell lines from PTPN12-expressing animals. Despite similar morphological appearances, however, PTPN12-deficient tumors and cell lines displayed increased expression of markers associated with the more aggressive basal-type breast cancer, i.e., SMA and keratin 5, and had decreased expression of the marker of the less aggressive luminal-type breast cancer, keratin 8. They also exhibited increased levels of several markers associated with EMT, such as Zeb1, Zeb2, N-cadherin, MMP-2, and cyclin D2. Aggressive tumors are known often to display features of EMT. Therefore, while not affecting the morphological appearance of tumors, loss of PTPN12 in ErbB2-dependent breast tumors elicited the appearance of features of more aggressive breast cancer.

Since primary tumors and lung metastases developed faster in mice lacking PTPN12, we tested whether this was due to enhanced cell proliferation, survival or both. While no effect on proliferation was observed, PTPN12-deficient primary tumors displayed a reduced frequency of cells having activated caspase 3, a marker of apoptosis. Similarly, cell lines devoid of PTPN12 had decreased susceptibility to anoikis, a form of anchorage-independent cell death. The latter finding is consistent with the observation that PTPN12 displayed enhanced features of EMT, which helps preserve survival of cells once they detach from their substratum. Thus, it is likely that loss of PTPN12 accelerated breast cancer development at least in part by preventing apoptosis and enhancing cell survival.

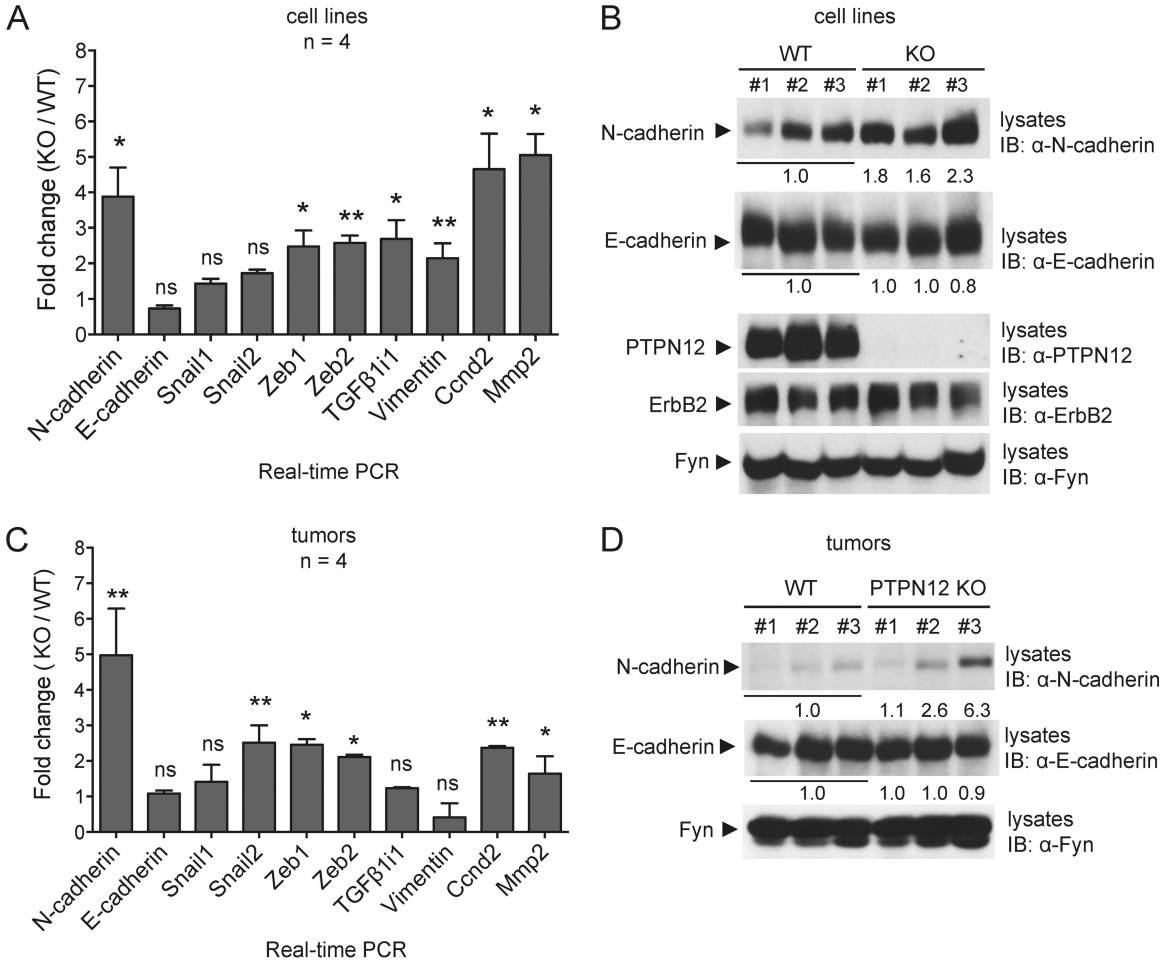

FIG 10 Expression of EMT markers in PTPN12-deficient tumors. (A) Expression of RNAs encoding the indicated epithelial-to-mesenchymal transition (EMT) markers was determined by real-time PCR. RNA samples from four different cell lines of each genotype were analyzed. Values were normalized using the housekeeping gene *Gapdh*. Average fold changes with standard deviations in PTPN12-deficient cells (knockout [KO]) compared to control cells (wild type [WT]) are depicted. **, $P < 0.01$; *, $P < 0.05$; ns, not significant. (B) Expression of EMT markers in tumor-derived cell lines was determined by immunoblot analyses. Representative cell lines are shown. Relative expression levels are shown at the bottom. (C) As for panel A, except that RNAs from primary tumors were analyzed. RNA samples from four tumors of each genotype were analyzed. (D) As for panel B, except that multiple independent primary tumors were analyzed. All panels are representative of at least three independent experiments.

The increased frequency of lung metastases in PTPN12-deficient animals also raised the possibility that loss of PTPN12 facilitated cell migration, invasiveness, or both. Compared to PTPN12-expressing breast cancer cells, cells lacking PTPN12 effectively demonstrated markedly increased migration and invasiveness. Whereas it is likely that the increased frequency of lung metastases was in part due to more rapid tumor development in PTPN12-deficient mice, these findings suggested that an augmented capacity to migrate and invade also played a role. Increased migration and invasiveness are typical features of basal-type breast cancer and EMT (33, 34).

Insights into the molecular mechanisms by which loss of PTPN12 promoted migration, invasiveness, resistance to anoikis, and partial EMT were gained by analyses of protein tyrosine phosphorylation. PTPN12-deficient breast cancer cells exhibited an increase in tyrosine phosphorylation of Cas, Pyk2, and paxillin, three known substrates of PTPN12 (4). No effect on ErbB2 was seen. These changes were seen both in primary tumors and in tumor-derived cell lines and were corrected by reexpression of PTPN12. A small increase in the activity of the downstream kinases p70S6K and GSK3β was also noted. While these kinases are not direct substrates of PTPN12, they are known downstream effectors of PTPN12-regulated substrates, including Cas (35).

Consequently, we postulate that loss of PTPN12 promoted migration, invasiveness, resistance to anoikis, and EMT in the MMTV-NIC model by deregulating Cas, Pyk2, and paxillin. In particular, Pyk2 is a cytoplasmic PTK that regulates migration through its capacity to phosphorylate substrates such as paxillin (30). Unfortunately, we were not able to address the role of Pyk2 (or Cas and paxillin) using small interfering RNAs, given the inefficiency of transduction of primary mouse breast cancer cell lines (data not shown). Nonetheless, when added to PTPN12-deficient breast cancer cells, a pharmacological inhibitor of Pyk2 caused a dose-dependent decrease in migration, as well as in tyrosine phosphorylation of Pyk2 and paxillin. Thus, deregulation of Pyk2 and, perhaps, paxillin likely played a role in the altered migration of PTPN12-deficient breast cancer cells. Although it remains to be clarified if Pyk2 and paxillin or, possibly, Cas played

a role in the increased resistance to anoikis and EMT caused by PTPN12 deficiency, it is noteworthy that previous work showed that Cas has a role in EMT (36, 37).

Whereas our findings generally supported those previously obtained by Sun et al. using human mammary epithelial cells (14), one noticeable difference was that we did not observe any impact of PTPN12 deficiency on tyrosine phosphorylation of ErbB2. One possibility is that the lack of an effect on ErbB2 in our study was due to the fact that a constitutively activated form of ErbB2 was used, whereas wild-type endogenous ErbB2 was studied by Sun et al. It is also possible that loss of PTPN12 has a more prominent effect on tyrosine phosphorylation of other receptors PTKs, such as EGFR and Met, which were not tested here. However, it should be pointed out that in most cell types studied so far, PTPN12 primarily acted on cytoskeletal regulators, such as Cas, Pyk2, and paxillin, rather than on receptor PTKs.

Although our findings and those of others collectively provide compelling evidence that PTPN12 is a tumor suppressor in human cancer, it is noteworthy that this conclusion was not supported by a study performed by Harris et al. (38). The latter group found that *PTPN12* RNA was more frequently elevated in TNBCs than other subtypes of human breast cancer. Others observed the opposite when PTPN12 protein expression was analyzed (14, 16, 17). In addition, Harris et al. observed that shRNA-mediated downregulation of PTPN12 expression caused diminished tumorigenicity and metastatic potential in established breast cancer cell lines. The opposite was found by us in the MMTV-NIC model and by Sun et al. (14) in human mammary epithelial cells. One issue with the study by Harris et al. is that expression of PTPN12 was studied only at the RNA level, not at the protein level. Perhaps *PTPN12* RNA levels are not predictive of the levels of PTPN12 protein in breast cancer cells, due to translational regulation or changes in protein stability. Moreover, Harris et al. examined the impact of loss of PTPN12 expression in established cell lines. It is conceivable that removal of PTPN12 has different impacts on tumor progression *in vivo* or in primary mammary epithelial cells compared to established tumor cell lines.

Combined, our findings suggest a possible mechanism by which loss of PTPN12 in humans would be associated with more aggressive breast cancer subtypes, such as TNBCs (14, 16, 17). We propose that loss of PTPN12 in breast cancer, which is initiated by oncogenic receptor PTKs (such as ErbB2), promotes tumor progression by shifting the profile of tumors toward that of more aggressive tumors. As the latter tumors frequently lose dependence on oncogenic receptor PTKs, such an evolution could explain why loss of PTPN12 is more commonly seen in TNBCs in humans. This could also be the case for other types of human cancer in which loss of PTPN12 is more often seen in aggressive subtypes. These include lung cancer, nasopharyngeal cancer, esophageal cancer, and hepatocellular carcinoma (14, 18, 20, 21).

In summary, we found that PTPN12 is a suppressor of breast cancer development and progression in an ErbB2-dependent mouse model of breast cancer. This function correlates with the ability of PTPN12 to dephosphorylate Cas, Pyk2, and paxillin, as well as its capacity to suppress EMT, migration, and cell survival. These findings support the idea that PTPN12 is a tumor suppressor in human breast cancer and, possibly, other types of human cancer. They enhance our understanding of the cellular and molecular mechanisms of action of PTPN12 in this setting. Lastly, they raise the possibility that targeting effectors of PTPN12-dependent tumor progression, such as the kinase Pyk2, using pharmacological inhibitors could be a useful modality in the treatment of certain types of human cancer.

ACKNOWLEDGMENTS

We thank the members of the Veillette lab for discussions.

This work was supported by grants from the Canadian Institutes of Health Research (CIHR) to A.V. N.W. is recipient of a Fellowship from Fonds de la Recherché du Québec—Santé (FRQS). A.V. holds the Canada Research Chair in Signaling in the Immune System.

J.L. planned experiments, performed experiments, interpreted data, and wrote the manuscript. D.D., C.M.S., and M.-C.Z. planned experiments, performed experiments, and interpreted data. N.W. and M.P. provided advice and interpreted data. W.J.M. provided critical reagents, provided advice, and interpreted data. A.V. planned experiments, generated reagents, interpreted data, wrote the manuscript, and obtained funding.

We declare no competing financial interests.

REFERENCES

1. **Tonks NK.** 2006. Protein tyrosine phosphatases: from genes, to function, to disease. Nat Rev Mol Cell Biol **7:**833–846.
2. **Pao LI, Badour K, Siminovitch KA, Neel BG.** 2007. Nonreceptor protein-tyrosine phosphatases in immune cell signaling. Annu Rev Immunol **25:**473–523. http://dx.doi.org/10.1146/annurev.immunol.23.021704.115647.
3. **Julien SG, Dube N, Hardy S, Tremblay ML.** 2011. Inside the human cancer tyrosine phosphatome. Nat Rev Cancer **11:**35–49. http://dx.doi.org/10.1038/nrc2980.
4. **Veillette A, Rhee I, Souza CM, Davidson D.** 2009. PEST family phosphatases in immunity, autoimmunity, and autoinflammatory disorders. Immunol Rev **228:**312–324. http://dx.doi.org/10.1111/j.1600-065X.2008.00747.x.
5. **Rhee I, Davidson D, Souza CM, Vacher J, Veillette A.** 2013. Macrophage fusion is controlled by the cytoplasmic protein tyrosine phosphatase PTP-PEST/PTPN12. Mol Cell Biol **33:**2458–2469. http://dx.doi.org/10.1128/MCB.00197-13.
6. **Souza CM, Davidson D, Rhee I, Gratton JP, Davis EC, Veillette A.** 2012. The phosphatase PTP-PEST/PTPN12 regulates endothelial cell migration and adhesion, but not permeability, and controls vascular development and embryonic viability. J Biol Chem **287:**43180–43190. http://dx.doi.org/10.1074/jbc.M112.387456.
7. **Davidson D, Shi X, Zhong MC, Rhee I, Veillette A.** 2010. The phosphatase PTP-PEST promotes secondary T cell responses by dephosphorylating the protein tyrosine kinase Pyk2. Immunity **33:**167–180. http://dx.doi.org/10.1016/j.immuni.2010.08.001.
8. **Rhee I, Zhong MC, Reizis B, Cheong C, Veillette A.** 2014. Control of dendritic cell migration, T cell-dependent immunity, and autoimmunity by protein tyrosine phosphatase PTPN12 expressed in dendritic cells. Mol Cell Biol **34:**888–899. http://dx.doi.org/10.1128/MCB.01369-13.
9. **Sirois J, Cote JF, Charest A, Uetani N, Bourdeau A, Duncan SA, Daniels E, Tremblay ML.** 2006. Essential function of PTP-PEST during mouse embryonic vascularization, mesenchyme formation, neurogenesis and early liver development. Mech Dev **123:**869–880. http://dx.doi.org/10.1016/j.mod.2006.08.011.
10. **Cote JF, Charest A, Wagner J, Tremblay ML.** 1998. Combination of gene targeting and substrate trapping to identify substrates of protein tyrosine phosphatases using PTP-PEST as a model. Biochemistry **37:**13128–13137. http://dx.doi.org/10.1021/bi981259l.
11. **Angers-Loustau A, Cote JF, Charest A, Dowbenko D, Spencer S, Lasky LA, Tremblay ML.** 1999. Protein tyrosine phosphatase-PEST regulates focal adhesion disassembly, migration, and cytokinesis in fibroblasts. J Cell Biol **144:**1019–1031. http://dx.doi.org/10.1083/jcb.144.5.1019.
12. **Charest A, Wagner J, Jacob S, McGlade CJ, Tremblay ML.** 1996. Phosphotyrosine-independent binding of SHC to the NPLH sequence of murine protein-tyrosine phosphatase-PEST. Evidence for extended phosphotyrosine binding/phosphotyrosine interaction domain recognition specificity. J Biol Chem **271:**8424–8429.
13. **Davidson D, Veillette A.** 2001. PTP-PEST, a scaffold protein tyrosine phosphatase, negatively regulates lymphocyte activation by targeting a unique set of substrates. EMBO J **20:**3414–3426. http://dx.doi.org/10.1093/emboj/20.13.3414.

14. **Sun T, Aceto N, Meerbrey KL, Kessler JD, Zhou C, Migliaccio I, Nguyen DX, Pavlova NN, Botero M, Huang J, Bernardi RJ, Schmitt E, Hu G, Li MZ, Dephoure N, Gygi SP, Rao M, Creighton CJ, Hilsenbeck SG, Shaw CA, Muzny D, Gibbs RA, Wheeler DA, Osborne CK, Schiff R, Bentires-Alj M, Elledge SJ, Westbrook TF.** 2011. Activation of multiple proto-oncogenic tyrosine kinases in breast cancer via loss of the PTPN12 phosphatase. Cell **144:**703–718. http://dx.doi.org/10.1016/j.cell.2011.02.003.
15. **Zheng Y, Zhang C, Croucher DR, Soliman MA, St-Denis N, Pasculescu A, Taylor L, Tate SA, Hardy WR, Colwill K, Dai AY, Bagshaw R, Dennis JW, Gingras AC, Daly RJ, Pawson T.** 2013. Temporal regulation of EGF signalling networks by the scaffold protein Shc1. Nature **499:**166–171. http://dx.doi.org/10.1038/nature12308.
16. **Xunyi Y, Zhentao Y, Dandan J, Funian L.** 2012. Clinicopathological significance of PTPN12 expression in human breast cancer. Braz J Med Biol Res **45:**1334–1340. http://dx.doi.org/10.1590/S0100-879X2012007500163.
17. **Wu MQ, Hu P, Gao J, Wei WD, Xiao XS, Tang HL, Li X, Ge QD, Jia WH, Liu RB, Xie XM.** 2013. Low expression of tyrosine-protein phosphatase nonreceptor type 12 is associated with lymph node metastasis and poor prognosis in operable triple-negative breast cancer. Asian Pac J Cancer Prev **14:**287–292. http://dx.doi.org/10.7314/APJCP.2013.14.1.287.
18. **Luo RZ, Cai PQ, Li M, Fu J, Zhang ZY, Chen JW, Cao Y, Yun JP, Xie D, Cai MY.** 2014. Decreased expression of PTPN12 correlates with tumor recurrence and poor survival of patients with hepatocellular carcinoma. PLoS One **9:**e85592. http://dx.doi.org/10.1371/journal.pone.0085592.
19. **Su Z, Tian H, Song HQ, Zhang R, Deng AM, Liu HW.** 2013. PTPN12 inhibits oral squamous epithelial carcinoma cell proliferation and invasion and can be used as a prognostic marker. Med Oncol **30:**618. http://dx.doi.org/10.1007/s12032-013-0618-4.
20. **Cao X, Chen YZ, Luo RZ, Zhang L, Zhang SL, Zeng J, Jiang YC, Han YJ, Wen ZS.** 2015. Tyrosine-protein phosphatase non-receptor type 12 expression is a good prognostic factor in resectable non-small cell lung cancer. Oncotarget **10:**11704–11713.
21. **Zhang XK, Xu M, Chen JW, Zhou F, Ling YH, Zhu CM, Yun JP, Cai MY, Luo RZ.** 2015. The prognostic significance of tyrosine-protein phosphatase nonreceptor type 12 expression in nasopharyngeal carcinoma. Tumour Biol **36:**5201–5208. http://dx.doi.org/10.1007/s13277-015-3176-x.
22. **Ursini-Siegel J, Hardy WR, Zuo D, Lam SH, Sanguin-Gendreau V, Cardiff RD, Pawson T, Muller WJ.** 2008. ShcA signalling is essential for tumour progression in mouse models of human breast cancer. EMBO J **27:**910–920. http://dx.doi.org/10.1038/emboj.2008.22.
23. **Brantley-Sieders DM, Zhuang G, Hicks D, Fang WB, Hwang Y, Cates JM, Coffman K, Jackson D, Bruckheimer E, Muraoka-Cook RS, Chen J.** 2008. The receptor tyrosine kinase EphA2 promotes mammary adenocarcinoma tumorigenesis and metastatic progression in mice by amplifying ErbB2 signaling. J Clin Invest **118:**64–78. http://dx.doi.org/10.1172/JCI33154.
24. **Perez-Quintero LA, Roncagalli R, Guo H, Latour S, Davidson D, Veillette A.** 2014. EAT-2, a SAP-like adaptor, controls NK cell activation through phospholipase Cgamma, Ca++, and Erk, leading to granule polarization. J Exp Med **211:**727–742. http://dx.doi.org/10.1084/jem.20132038.
25. **Veillette A, Bookman MA, Horak EM, Bolen JB.** 1988. The CD4 and CD8 T cell surface antigens are associated with the internal membrane tyrosine-protein kinase p56lck. Cell **55:**301–308. http://dx.doi.org/10.1016/0092-8674(88)90053-0.
26. **Buckbinder L, Crawford DT, Qi H, Ke HZ, Olson LM, Long KR, Bonnette PC, Baumann AP, Hambor JE, WAGrasser 3rd, Pan LC, Owen TA, Luzzio MJ, Hulford CA, Gebhard DF, Paralkar VM, Simmons HA, Kath JC, Roberts WG, Smock SL, Guzman-Perez A, Brown TA, Li M.** 2007. Proline-rich tyrosine kinase 2 regulates osteoprogenitor cells and bone formation, and offers an anabolic treatment approach for osteoporosis. Proc Natl Acad Sci U S A **104:**10619–10624. http://dx.doi.org/10.1073/pnas.0701421104.
27. **Schade B, Rao T, Dourdin N, Lesurf R, Hallett M, Cardiff RD, Muller WJ.** 2009. PTEN deficiency in a luminal ErbB-2 mouse model results in dramatic acceleration of mammary tumorigenesis and metastasis. J Biol Chem **284:**19018–19026. http://dx.doi.org/10.1074/jbc.M109.018937.
28. **Marcotte R, Smith HW, Sanguin-Gendreau V, McDonough RV, Muller WJ.** 2012. Mammary epithelial-specific disruption of c-Src impairs cell cycle progression and tumorigenesis. Proc Natl Acad Sci U S A **109:**2808–2813. http://dx.doi.org/10.1073/pnas.1018861108.
29. **Taddei ML, Giannoni E, Fiaschi T, Chiarugi P.** 2012. Anoikis: an emerging hallmark in health and diseases. J Pathol **226:**380–393. http://dx.doi.org/10.1002/path.3000.
30. **Schaller MD.** 2010. Cellular functions of FAK kinases: insight into molecular mechanisms and novel functions. J Cell Sci **123:**1007–1013. http://dx.doi.org/10.1242/jcs.045112.
31. **Perou CM, Sorlie T, Eisen MB, van de Rijn M, Jeffrey SS, Rees CA, Pollack JR, Ross DT, Johnsen H, Akslen LA, Fluge O, Pergamenschikov A, Williams C, Zhu SX, Lonning PE, Borresen-Dale AL, Brown PO, Botstein D.** 2000. Molecular portraits of human breast tumours. Nature **406:**747–752. http://dx.doi.org/10.1038/35021093.
32. **Sorlie T, Perou CM, Tibshirani R, Aas T, Geisler S, Johnsen H, Hastie T, Eisen MB, van de Rijn M, Jeffrey SS, Thorsen T, Quist H, Matese JC, Brown PO, Botstein D, Lonning PE, Borresen-Dale AL.** 2001. Gene expression patterns of breast carcinomas distinguish tumor subclasses with clinical implications. Proc Natl Acad Sci U S A **98:**10869–10874. http://dx.doi.org/10.1073/pnas.191367098.
33. **Sarrio D, Rodriguez-Pinilla SM, Hardisson D, Cano A, Moreno-Bueno G, Palacios J.** 2008. Epithelial-mesenchymal transition in breast cancer relates to the basal-like phenotype. Cancer Res **68:**989–997. http://dx.doi.org/10.1158/0008-5472.CAN-07-2017.
34. **Lamouille S, Xu J, Derynck R.** 2014. Molecular mechanisms of epithelial-mesenchymal transition. Nat Rev Mol Cell Biol **15:**178–196. http://dx.doi.org/10.1038/nrm3758.
35. **Wallez Y, Mace PD, Pasquale EB, Riedl SJ.** 2012. NSP-CAS protein complexes: emerging signaling modules in cancer. Genes Cancer **3:**382–393. http://dx.doi.org/10.1177/1947601912460050.
36. **Bisaro B, Montani M, Konstantinidou G, Marchini C, Pietrella L, Iezzi M, Galie M, Orso F, Camporeale A, Colombo SM, Di Stefano P, Tornillo G, Camacho-Leal MP, Turco E, Taverna D, Cabodi S, Amici A, Defilippi P.** 2012. p130Cas/Cyclooxygenase-2 axis in the control of mesenchymal plasticity of breast cancer cells. Breast Cancer Res **14:**R137. http://dx.doi.org/10.1186/bcr3342.
37. **Tornillo G, Defilippi P, Cabodi S.** 2014. Cas proteins: dodgy scaffolding in breast cancer. Breast Cancer Res **16:**443. http://dx.doi.org/10.1186/s13058-014-0443-5.
38. **Harris IS, Blaser H, Moreno J, Treloar AE, Gorrini C, Sasaki M, Mason JM, Knobbe CB, Rufini A, Halle M, Elia AJ, Wakeham A, Tremblay ML, Melino G, Done S, Mak TW.** 2014. PTPN12 promotes resistance to oxidative stress and supports tumorigenesis by regulating FOXO signaling. Oncogene **33:**1047–1054. http://dx.doi.org/10.1038/onc.2013.24.